Available online at www.sciencedirect.com
SCIENCE DIRECT®
Journal of Hydrology 281 (2003) 96–114
Journal of Hydrology
www.elsevier.com/locate/jhydrol

Stream depletion predictions using pumping test data from a heterogeneous stream–aquifer system (a case study from the Great Plains, USA)

Stefan J. Kollet*, Vitaly A. Zlotnik

Department of Geosciences, University of Nebraska-Lincoln, 214 Bessey Hall, Lincoln, NE 68588, USA

Received 10 May 2002; accepted 1 May 2003

Abstract

This uniquely designed study investigates a fundamental issue—the feasibility of predicting stream depletion rates using linear uniform two-dimensional models. Required input for these models includes the hydraulic parameter estimates of the aquifer and the stream–aquifer interface, which may be obtainable through pumping test data analysis. This study utilizes pumping test data collected near the naturally meandering Prairie Creek, Platte River watershed, Nebraska, USA. Drawdown data were obtained in eight piezometer clusters, located on both sides of the stream, each containing three piezometers screened at different aquifer depths. Parameter estimates and, thus, stream depletion predictions varied over a wide range. Large parameter variance and a low degree of goodness of fit between the calculated and measured data encountered during the analysis suggest deficiencies of the uniform aquifer models in describing significant physical processes. This was also shown by additional field experiments that indicate lateral and vertical aquifer heterogeneity. Hydrogeological and sedimentological considerations of the meandering stream architecture (point bar versus cut bank) and the application of a linear piecewise-homogeneous model yielded a higher degree of goodness of fit and higher confidence in stream depletion predictions. Aquifer heterogeneity appears to be the major reason for uncertainty in stream depletion predictions, though other possible sources of uncertainty should be considered. These include the model linearity, the Dupuit assumption, the simplified representation of the stream–aquifer interface, the approximation of the stream as a straight line or a strip, and the impact of regional groundwater flow.

Keywords: Stream depletion; Pumping test; Parameter identification; Aquifer heterogeneity; Meandering stream; Sedimentologic information

1. Introduction

1.1. Theory of stream depletion

The pumping-induced stream depletion is defined as the reduction of streamflow due to induced infiltration of stream water into the aquifer and

* Corresponding author. Tel.: +1-402-472-2663; fax: +1-402-472-4917.
E-mail addresses: skollet@unlserve.unl.edu (S.J. Kollet), vzlotnik1@unlnotes.unl.edu (V.A. Zlotnik).

0022-1694/03/$ - see front matter © 2003 Elsevier B.V. All rights reserved.
doi:10.1016/S0022-1694(03)00203-8

capture of aquifer discharge to the stream (Theis, 1941; Bredehoeft, 1997; Sophocleous, 1997).

A number of linear two-dimensional mathematical models for estimating the stream depletion rate in the case of a fully penetrating stream and pumping well have been developed (Theis, 1941; Glover and Balmer, 1954; Hantush, 1965; Jenkins, 1968). More realistic representation of stream–aquifer systems incorporated the partial stream penetration (Hunt, 1999) and a finite stream width (Zlotnik and Huang, 1999; Zlotnik et al., 1999; Butler et al., 2001).

Yet, the conceptual streambed model introduced by Hantush (1965) inherent in most of these theoretical approaches represents the stream–aquifer interface as a continuous streambed of uniform thickness (m') and hydraulic conductivity (K'). This common groundwater flow modeling approach (Anderson and Woessner, 1992) simplifies the fundamental knowledge about the sedimentology of alluvial deposits (Bridge and Jarvis, 1976). Furthermore, the assumptions of horizontal groundwater flow (Dupuit assumption) and aquifer uniformity in these models have limited applicability in natural systems. And finally, these models neglect the sinuosity of meandering streams.

The hydraulic aquifer and streambed properties can be obtained from the drawdown analyses of pumping tests in the vicinity of the stream. Since the feasibility of stream depletion predictions is determined by parameter estimates, sensitivity of these models to various input parameters is paramount for the assessment of such models.

An important theoretical approach to the parameters sensitivities and correlations was suggested by Christensen (2000). Using the two-dimensional Hunt (1999) model, the study investigated the viability of unbiased estimates of the aquifer and streambed hydraulic properties. It was demonstrated that the location of drawdown measurements in the aquifer must be chosen carefully, and that it might not be possible to obtain accurate estimates of all parameters simultaneously. Additionally, pumping durations have to be long, and in some cases, depending on the encountered hydraulic properties and test geometry, they may be unrealistically long.

Since the stream depletion estimates are model dependent, several numerical studies evaluated the parameters' sensitivity and assessed the impact of various assumptions, which are most likely to be violated under real conditions (Spalding and Khaleel, 1991; Sophocleous et al., 1995; Conrad and Beljin, 1996; Butler et al., 2001). These factors are listed in decreasing order of potency as follows: (1) streambed conductance; (2) degree of aquifer penetration by the stream; (3) horizontal groundwater flow (Dupuit assumption); (4) uniformity of the aquifer; (5) degree of aquifer penetration by the pumping well.

1.2. Experimental studies of stream depletion

Accurate experimental data on stream depletion rates, which could be utilized in the assessment of physical concepts and mathematical models, constitute the fundamental difficulty of stream depletion studies in natural systems. Conceptually, the effects of stream depletion can be estimated by comparing the stream discharge between an upstream and a downstream cross-section near the pumping well. The difference between the upstream discharge, Q_{up}, and downstream discharge, Q_{down}, is referred to as the differential stream discharge $\Delta Q_s = Q_{up} - Q_{down}$ and is equivalent to the stream depletion rate along that particular stream reach of finite length.

If the accuracy of the ΔQ_s measurements significantly exceeds the stream depletion rate, the impact of nearby pumping on the stream discharge is objectively detectable and quantifiable. Yet, the pumping rate from a single well is commonly on the order of or below 0.01 m^3/s, while streamflow rates on the order of 1 m^3/s are not uncommon. Thus, even with the assumption that all the pumped water stems directly from the stream and a typical accuracy of about 5% for streamflow measurements in natural channels, an accurate streamflow and stream depletion rate assessment is obviously not feasible. Diurnal discharge variations further reduce the possibility of direct assessment of stream depletion rates.

Unfortunately, field experiments that could be utilized in the assessment of various models are limited in scope. During an early field study by Moore (1966), the hydraulic connection between the stream and the aquifer was lost and a variable saturation zone developed underneath the stream. Sophocleous et al. (1988) dealt with a two-aquifer system, where a relatively continuous clay layer separated two

interconnected aquifers. The pumping well was located in the lower aquifer, and the stream with shallow penetration was in the upper aquifer. However, the special case of a two-aquifer system is not the subject of the aforementioned mathematical models and must be treated separately.

Recently, Hunt et al. (2001) performed a pumping test along an engineered stream (ditch) with a streamflow rate of less than 0.05 m^3/s. Scarce information on the geology and hydrostratigraphy and the unusually low streamflow rate make the evaluation and transfer of their results to other alluvial stream–aquifer systems difficult. Nyholm et al. (2002) presented results from a field study on the watershed scale supplemented with numerical analysis. Although, only few results are shown from the application of analytical models, Nyholm et al. (2002) remark that these models tend to overestimate stream depletion. Design of these studies does not explicitly take into account the three-dimensional groundwater flow structure.

1.3. Goal and objectives

The goal of this study is to investigate the feasibility of parameter identification and stream depletion predictions from pumping test data by applying linear two-dimensional models of surface–groundwater interactions under pumping conditions. In this paper, emphasis is placed upon the

- comprehensive analysis of data from a long-term pumping test performed at the Prairie Creek test site using a three-dimensional piezometer network;
- description of different analysis strategies and sedimentologic concepts that were used in an attempt to obtain and improve parameter and stream depletion estimates;
- evaluation of assumptions made in the applied linear two-dimensional models.

2. Theory

2.1. General problem statement

We consider horizontal two-dimensional groundwater flow in an aquifer with the horizontal aquifer base as a reference level. The hydraulic head $h(x, y, t)$ and the stream stage $H(x, y, t)$ with the same reference level are described by the following boundary value problem (Fig. 1):

$$S\frac{\partial h}{\partial t} = \frac{\partial}{\partial x}\left(T\frac{\partial h}{\partial x}\right) + \frac{\partial}{\partial y}\left(T\frac{\partial h}{\partial y}\right) + g(H-h) + R - Q\delta(x-x_0)\delta(y-y_0), \qquad (x,y)\in\Omega, \tag{1}$$

$$h(x, y, 0) = h_\Omega(x, y), \qquad (x, y) \in \Omega, \tag{2}$$

$$h(x, y, t) = h_\Gamma(x, y, t), \qquad (x, y) \in \Gamma. \tag{3}$$

Here, x and y are Cartesian coordinates; t is time; $S(x, y)$ is storativity; $T(x, y)$ is transmissivity; $R(x, y)$ is the general groundwater recharge/discharge term; Q is the pumping rate of a well with coordinates (x_0, y_0); $g(x, y, t)$ is the streambed characteristic of the water exchange between the stream and groundwater in the domain Π beneath the stream; $h_\Omega(x, y)$ is the initial head distribution in the aquifer; Ω is the groundwater flow domain with boundary Γ; $h_\Gamma(x, y, t)$ is the known head at the boundary Γ; $\delta(x)$ is the Dirac function. (In certain cases, a known flux or other

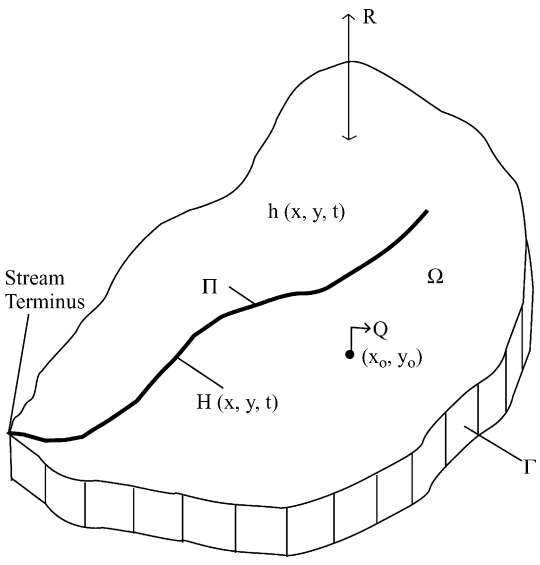

Fig. 1. Schematic two-dimensional diagram of a groundwater watershed.

conditions may be assigned at various parts of the boundary Γ.)

The above boundary value problem and its solutions are based on the Dupuit assumption and on the assumption of linearity. The Dupuit assumption implies the neglect of vertical flow, and the linearity assumption assumes that any change in saturated thickness is small compared to the initial saturated thickness, i.e. the aquifer saturated thickness, m, is constant.

Due to the linearity of the boundary value problem, the solution can be represented as the superposition of three terms

$$h(x,y,t) = h_b(x,y,t) - s_Q(x,y,t) + s_H(x,y,t), \qquad (4)$$

where the hydraulic head $h_b(x,y,t)$ describes the groundwater flow that corresponds to the baseflow conditions without pumping or bank storage effects ($Q=0$, $R\neq 0$, $H=\text{const}$); the drawdown term $s_Q(x,y,t)$ is due to pumping ($Q>0$, $R=0$, $H=\text{const}$); and the drawdown term $s_H(x,y,t)$ is due to bank storage effects ($Q=0$, $R=0$, $H\neq\text{const}$). Here, $s_Q(x,y,t)>0$ for $Q>0$ and $s_H(x,y,t)>0$ for $dH/dt>0$.

In our study, sinuosity of the stream and spatial variations of the stream stage are neglected, and an alluvial valley of infinite width is considered as shown in Fig. 2 (Zlotnik and Huang, 1999; Zlotnik et al., 1999). Considering a finite stream width W and lateral variability of aquifer properties (Butler et al., 2001),

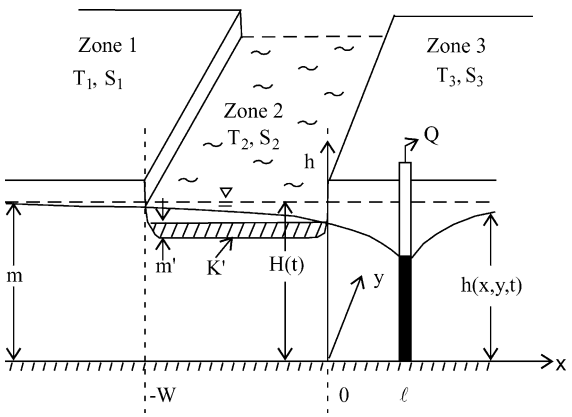

Fig. 2. Schematic hydrogeologic conditions of stream–aquifer interactions under pumping conditions.

the initial boundary value problem (1)–(3) can be simplified as follows

$$S\frac{\partial h}{\partial t} = \frac{\partial}{\partial x}\left(T\frac{\partial h}{\partial x}\right) + \frac{\partial}{\partial y}\left(T\frac{\partial h}{\partial y}\right) + g(H-h) + R - Q\delta(x-\ell)\delta(y), \quad |x|<\infty,\ |y|<\infty, \qquad (5)$$

$$h(x,y,0) = m, \qquad (6)$$

$$h(x,y,t) = m, \quad x^2+y^2 \to \infty, \qquad (7)$$

$$H(x,y,t) = H(t) = m, \quad -W < x < 0, \qquad (8)$$

where m is the aquifer saturated thickness. Aquifer parameters may vary laterally between the stream banks and the sub-stream zone (Fig. 2), thus:

$$S(x,y) = \begin{cases} S_1, & x<-W; \\ S_2, & -W<x<0; \\ S_3, & x>0; \end{cases}$$
$$T(x,y) = \begin{cases} K_1m_1, & x<-W; \\ K_2m_2, & -W<x<0; \\ K_3m_3, & x>0; \end{cases} \qquad (9)$$

$$g(x,y) = \begin{cases} 0, & x<-W; \\ K'/m', & -W<x<0; \\ 0, & x>0; \end{cases}$$
$$m(x,y) = \begin{cases} m_1, & x<-W; \\ m_2, & -W<x<0; \\ m_3, & x>0; \end{cases} \qquad (10)$$

K_i is the hydraulic conductivity, m_i is the saturated thickness, $T_i = K_i m_i$ is the transmissivity, Si is the storativity of the ith zone, where $i=1,2,$ or 3. K' and m' are the hydraulic conductivity and the thickness of the streambed, respectively; the ratio K'/m' is the streambed conductance per unit streambed area; ℓ is the distance from the well to the stream bank. The hydraulic head and flux are continuous along the interfaces between Zones 1, 2, and 3 (lines $x=0$ and $x=-W$).

It is important to note that during a pumping test that lasts for several days, the temporal variability of the hydraulic head due to changes in baseflow conditions $h_b(x,y,t)$ is usually neglected, and only measurable drawdown $s(x,y,t)$

due to pumping and stream stage fluctuations is considered:

$$s(x,y,t) = s_Q(x,y,t) - s_H(x,y,t). \tag{11}$$

The stream depletion rate $q(t)$ is entirely determined by pumping-induced head changes $s_Q(x,y,t)$ under the streambed, and quantitative evaluation of stream depletion rate is based upon the summation of induced seepage through the streambed (Zlotnik et al., 1999; Butler et al., 2001):

$$q(t) = \int_{-\infty}^{+\infty}\int_{-W}^{0} \frac{K'}{m'} s_Q \,\mathrm{d}x\mathrm{d}y. \tag{12}$$

Solution of the boundary value problem (5)–(10) yields a head distribution, which can be substituted into Eq. (12) for the estimation of the stream depletion rate. Aquifer parameters required for such estimates must be obtained from the interpretation of the drawdown record $s(x,y,t)$ from pumping tests.

2.2. Hydraulic head dynamics on the watershed

Simulation of transient hydraulic head includes the prediction of baseflow conditions, $h_b(x,y,t)$, on a large time scale (months) that are related to a poorly identifiable recharge R. It is common to separate relatively short-term observable effects of bank storage processes and pumping (terms $s_H(x,y,t)$ and $s_Q(x,y,t)$ in Eqs. (4) and (11), respectively) from the long-term baseflow-related head changes and treat each term separately. The water level response to stream stage fluctuations $s_H(x,y,t)$ can be obtained considering $Q = 0$ and $R = 0$, and pumping-induced head changes $s_Q(x,y,t)$ are derived assuming $R = 0$ and $H = \text{const}$ using different versions of the boundary value problem (5)–(10).

This separation is especially important in experimental delineation of stream depletion. During the process of pumping, changes of the stream stage, s_H (Eqs. (4) and (11)) can affect the observed drawdown, and bank storage effects should be considered. In our study, bank storage effects had only little influence upon measured drawdowns, as the analysis with the linear model by Zlotnik and Huang (1999) for water level responses to stream stage fluctuations revealed. Yet, this finding cannot be readily transferred to other possible cases, thus, bank storage effects should always undergo case-specific evaluation.

Zlotnik et al. (1999) presented the general framework for investigating the effects of pumping near a stream in a wide alluvial valley using Eqs. (5)–(10). Butler et al. (2001) extended the problem statement for large-scale heterogeneity and finite alluvial valley width. This semi-analytical method (BZT model) was implemented in a Fortran code by Butler and Tsou (1999). It was numerically shown that this approach has a good accuracy for anisotropic conditions and various degrees of aquifer penetration by the stream.

Simultaneously, Hunt (1999) investigated a stream of zero width (line source). In this case, the pumping-induced head changes can be reduced to a simple functional form (the notation of the original publications is purposely preserved):

$$s_Q(x,y,t) = \frac{Q}{4\pi T}\left\{E_1\left[\frac{(\ell - x)^2 + y^2}{4Tt/S}\right] - \int_0^{\infty} \mathrm{e}^{-\theta} E_1\left[\frac{(\ell + |x| + 2T\theta/\lambda)^2 + y^2}{4Tt/S}\right]\mathrm{d}\theta\right\},$$
$$(-\infty < x > \infty,\ -\infty < y > \infty,\ 0 < t > \infty), \tag{13}$$

where λ was some undefined leakance parameter for the streambed. Later, Hunt et al. (2001) relaxed the requirement of zero stream width. Using a qualitative analysis, they hypothesized that λ can be expressed through K'/m' and W as follows:

$$\lambda \approx W\frac{K'}{m'}. \tag{14}$$

It was found that the Hunt and BZT models provide almost identical drawdown and stream depletion for our system's geometry. Hunt et al. (2001) hypothesized that if $\ell/W \gg 1$, a stream of finite width can be readily approximated by a line source. In our case the ratio is $\ell/W = 5.7$. Because it was computationally less extensive, we applied the Hunt model of uniform aquifer conditions for nonlinear parameter optimization. The more general BZT model was used during the discussion of the influence of large-scale aquifer heterogeneity.

2.3. Pumping-induced stream depletion

Currently, there exist four analytical approaches for the prediction of stream depletion that are based upon the following assumptions: (1) the stream fully penetrates the uniform aquifer and the streambed and aquifer have identical hydraulic conductivity (Theis, 1941); (2) the stream fully penetrates the uniform aquifer and the aquifer and vertical stream–aquifer interface have contrasting hydraulic conductivities (Hantush, 1965); (3) the stream is shallow, and the uniform aquifer and horizontal stream–aquifer interface have contrasting hydraulic conductivities (Zlotnik et al., 1999; Hunt, 1999); (4) the stream is shallow and the nonuniform aquifer and horizontal interface have contrasting hydraulic conductivity values (Butler et al., 2001). The latter will be called the BZT model for brevity.

The first realistic presentation of streambed geometry by Zlotnik et al. (1999) was based upon a three-zone approach as shown in Fig. 2. For a shallow stream the results of Zlotnik et al. (1999, Eqs. (11) and (12)) can be presented as follows

$$\frac{q(t)}{Q} = D\left(\frac{t}{t_a}, \frac{l}{B_S}\right),$$
$$D(u,v) = \operatorname{erfc}\left(\frac{1}{2\sqrt{u}}\right) - e^{v^2u+v}\operatorname{erfc}\left(\frac{1}{2\sqrt{u}} + v\sqrt{u}\right), \tag{15}$$

$$t_a = \frac{S\ell^2}{T}, \qquad B_S = B\coth\frac{W}{2B},$$
$$B = \sqrt{\frac{m'T}{K'}}, \qquad \coth x = \frac{e^x + e^{-x}}{e^x - e^{-x}}, \tag{16}$$

where B_S is the streambed conductance coefficient.

It is assumed that storativity S and transmissivity T are uniform over the alluvial aquifer. Zlotnik et al. (1999) showed that neglecting the compressibility of the sub-stream zone is a valid assumption.

For the special case of a small stream width ($W \ll 2B$),

$$B_S \approx \frac{2m'T}{WK'} = \frac{2T}{\lambda}, \qquad \lambda = W\frac{K'}{m'}, \tag{17}$$

and Eq. (15) reduces to the solution for stream depletion derived by Hunt (1999, Eq. (20)).

These expressions need generalization for the application to a nonuniform aquifer. In this case the semi-analytical BZT model for the stream depletion rate calculations can be utilized (Butler and Tsou, 1999).

3. Test site hydrology and hydrogeology

The test site is located along a meander of the Prairie Creek, east-central Nebraska, Platte River watershed, Great Plains, USA (Fig. 3). Prairie Creek drains an area of approximately 250 km^2, typical for Platte River tributaries in that region. It originates about 1.5 km northwest of Grand Island, Nebraska and meanders eastward more or less parallel to the Platte River. The confluence with the Platte River is located about 4.5 km east of the test site. At the study site the stream channel is 20 m wide and penetrates the aquifer by less than 5%. Records indicate that streamflow varies from 0 m^3/s under drought conditions to 50 m^3/s during the spring in some years. During the experiment that was performed under low-flow conditions, the average active channel width and stream discharge was 10 m and 0.25 m^3/s, respectively.

Groundwater constantly enters the area as ambient flow from adjacent areas to the northwest. Further downgradient, groundwater flow is mainly eastward and parallel to the Platte River in the study area.

At the test site, the unconfined aquifer underlying the Prairie Creek consists of unconsolidated alluvium that has an average saturated thickness of about 17 m and comprises poorly sorted sand and gravely material of Quaternary age (Fig. 3). The sediments are of continental origin and were deposited in paleochannels of the Platte River. At the top, recent deposits from the Prairie Creek are distinguishable by morphological features and consist of reworked paleoalluvium of the Platte River. In this paper, we refer to the northwest bank as the point bar and to the southeast bank as the cut bank, which is consistent with the sedimentologic framework at the site. The streambed sediments mainly consist of coarse sand and fine

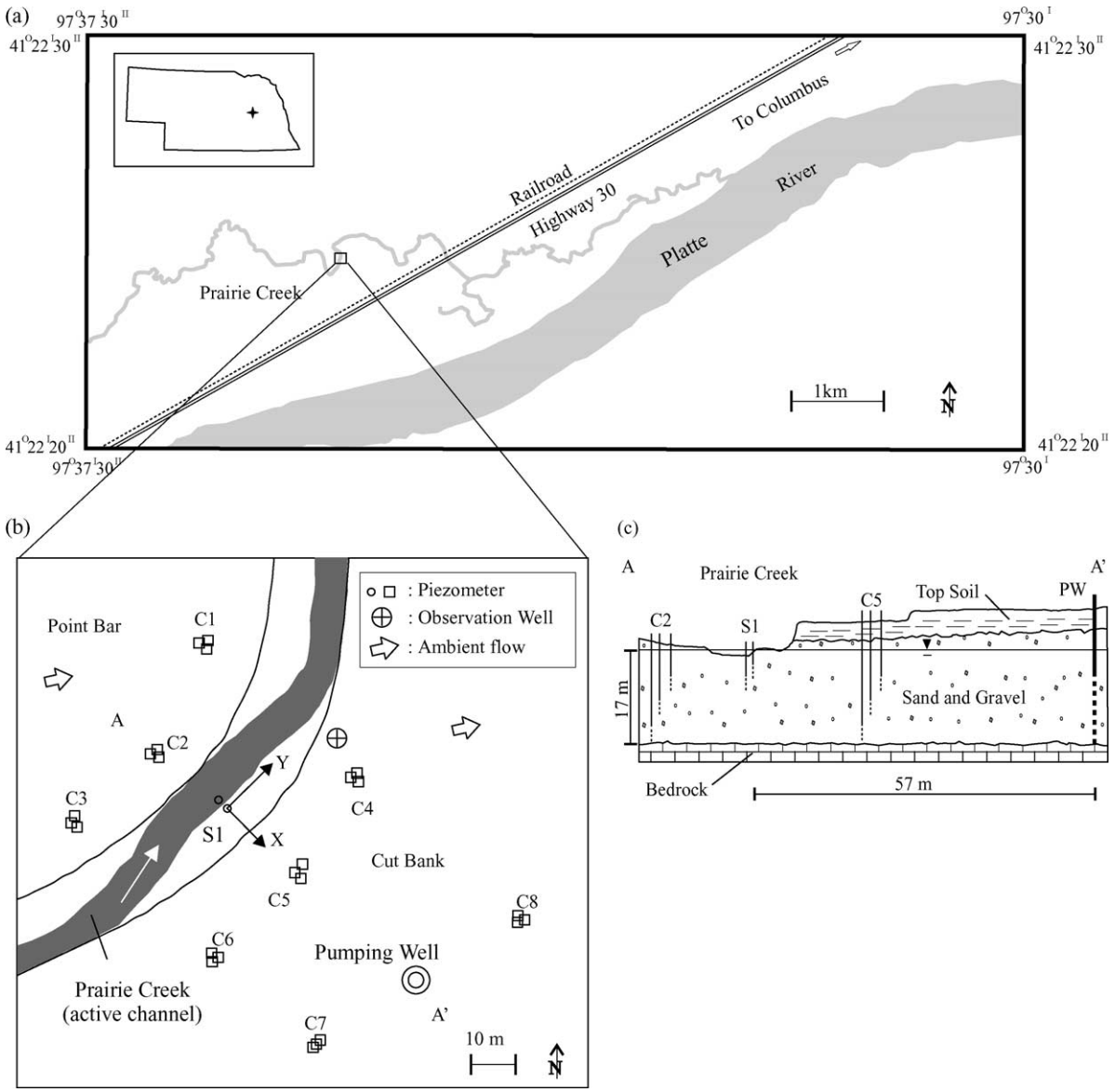

Fig. 3. Prairie Creek test site in Nebraska, USA: (a) location, (b) instrumentation, and (c) conceptual hydrogeologic cross-section (not in scale). Note the origin of coordinates (Table 1). Shaded area in (b) indicates the active channel. The cross-section shows boundaries of the hydrogeologic units, positions of the piezometer screens and the pumping well (PW).

gravel and have an effective vertical hydraulic conductivity of about $K' = 18$ m/day (Cardenas and Zlotnik, 2003). The bedrock at the bottom of the aquifer consists of a continuous clay layer of Cretaceous age (Sniegocki, 1955; Peckenpaugh and Dugan, 1983).

4. Methodology

4.1. Site instrumentation and data collection

The test site (Fig. 3) has a high capacity pumping well, eight piezometer clusters, and a 10-cm-diameter

observation well penetrating about 90% of the saturated aquifer thickness at a distance of 3 m from the cut bank. The pumping well is completed at the aquifer base at a depth of about 19.5 m with a casing diameter of 40 cm at a distance of 57 m from the stream. The screened interval extends from about 4.9 to 19.5 m aquifer depth and covers about 78% of the saturated aquifer thickness under nonpumping conditions.

Each individual piezometer cluster includes three piezometers 5 cm in diameter that are screened at shallow (~4.6 m), intermediate (~9.5 m), and deep (~19 m) aquifer depths. Two additional piezometers (cluster S1) are located in the center of the stream channel along the main transect A–A′ and completed at depths 1.2 and 4.1 m. The screen length of each piezometer is 76 cm. A stream stage and water temperature measurement point is located at the stream bank in deeper channel parts at a distance of about 50 m upstream from the main transect.

All depths values provided above were measured from the ground surface. The Cartesian coordinates following the convention by Zlotnik et al. (1999) and Butler et al. (2001), shown in Fig. 2, and the distances from the initial water table to the screen bottom of the piezometers are given in Table 1. In the following sections, shallow, intermediate, and deep completion depths are indicated with the extensions s, i, and d, respectively (e.g. C1s: shallow piezometer in cluster C1).

The pumping test started on May 30, 2000 and continued for 144 h. The pumping rate was held constant at 6480 m^3/day and was monitored continuously. The pumped water was discharged into the stream about 300 m downstream from the site. The pumping test data set includes hydraulic head data, collected at all the monitoring points in the aquifer; groundwater temperature data, collected in nine piezometers; and continuous stream stage and water temperature data (2 min sampling rate). In 11 piezometers, the head and temperature data were taken automatically via pressure–temperature transducers connected to two data logger units (2 and 5 min sampling rates). Data from the remaining 15 piezometers and the 10-cm-diameter well were measured manually.

4.2. Pumping test data analysis

4.2.1. Correspondence between 3D field data and 2D models

Differences in the piezometer head responses at different locations in the aquifer (Fig. 4) are representative of the three-dimensional nature of the groundwater flow field of the stream–aquifer system. In order to apply the two-dimensional groundwater flow models that are based on the Dupuit and linearity assumptions it is necessary to vertically average the drawdown, $s(x, y, z, t)$, across the saturated thickness at each cluster location (x, y)

Table 1
Well coordinates and depths to the screen bottom from the initial water table on May 30, (2000)

Well	Parameters			Well	Parameters			Well	Parameters		
	x (m)	y (m)	Depth (m) to screen bottom		x (m)	y (m)	Depth (m) to screen bottom		x (m)	y (m)	Depth (m) to screen bottom
C1s	−27.3	24.6	3.4	C4s	16.1	25.0	2.8	C7s	48.1	−23.6	1.9
C1i	−27.4	24.0	7.5	C4i	16.6	24.7	7.7	C7i	48.2	−22.7	7.4
C1d	−27.1	24.2	17.1	C4d	16.1	24.3	17.0	C7d	48.3	−21.8	16.6
C2s	−19.3	0.0	3.0	C5s	21.3	2.9	2.8	C8s	62.8	26.5	2.4
C2i	−18.3	1.0	7.2	C5i	20.7	2.1	7.0	C8i	62.7	27.1	7.4
C2d	−18.9	−0.3	16.5	C5d	20.8	3.3	17.2	C8d	62.1	26.6	16.9
C3s	−22.3	−22.4	2.7	C6s	20.8	−23.1	2.3	S1s	−0.3	2.3	1.2
C3i	−21.8	−22.5	7.0	C6i	20.6	−23.6	7.1	S1d	0.0	2.3	4.1
C3d	−21.9	−22.0	15.4	C6d	20.1	−23.2	15.8	10-cm	7.1	28.8	15.6

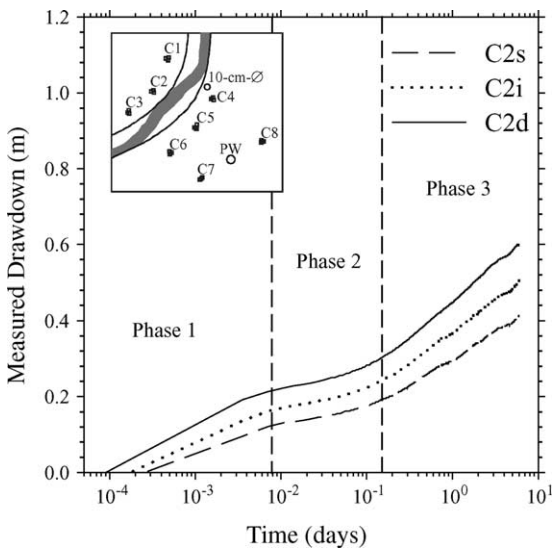

Fig. 4. Example of the typical time–drawdown behavior in an unconfined aquifer exhibiting three distinct phases. Data were measured in the piezometers of cluster C2 at the point bar.

to obtain a two-dimensional head distribution, $s_{av}(x, y, t)$

$$s_{av}(x, y, t) = \frac{1}{m} \int_0^m s(x, y, z, t)\mathrm{d}z, \tag{18}$$

where m is the aquifer saturated thickness.

The discrete form of Eq. (18) for our test geometry is as follows

$$s_{av}(x, y, t) = s_s f_s + s_i f_i + s_d f_d, \tag{19}$$

$$f_s = \left[d_s + \left(\frac{d_i - d_s}{2} \right) \right] / m;$$

$$f_i = \left[\left(\frac{d_i - d_s}{2} \right) + \left(\frac{d_d - d_i}{2} \right) \right] / m; \tag{20}$$

$$f_d = \left[\left(\frac{d_d - d_i}{2} \right) \right] / m,$$

where s_s, s_i, and s_d are the measured drawdowns in the shallow, intermediate and deep piezometers, respectively; d_s, d_i, and d_d are the depths of the screens below the initial water table of the shallow, intermediate and deep piezometers, respectively; f_s, f_i, and f_d are the respective weighting coefficients. Note that the deep piezometers were completed at the aquifer base.

4.2.2. Grouping of piezometer clusters data for analyses

The averaged time–drawdown data were analyzed in different groups:

1. *Individual clusters analyses, ICA.* Individual analysis of the data from each piezometer cluster and the 10-cm-diameter observation well. The ICA yields a total of nine parameter vectors.
2. *Bank clusters analyses, BCA.* Analysis of the data from the point bar and the cut bank. The BCA yields a total of two parameter vectors by utilizing the time–drawdown data from the clusters C1, C2, C3 (point bar) and C4, C5, C6, C7, C8 (cut bank) simultaneously.
3. *Global clusters analysis, GCA.* Simultaneous analysis of the data from all piezometer clusters, C1 to C8. The GCA yields a single parameter vector.

For consistency, the data collected in the 10-cm-diameter observation well were not included into the BCA and GCA. Data from the two-piezometer cluster in the stream, S1, were not utilized either.

4.2.3. Parameter identification

Streambed and aquifer parameters were determined using constant values for the pumping rate, $Q = 6480\ \mathrm{m}^3/\mathrm{day}$; distance to the well, $\ell = 57$ m; and stream width, $W = 10$ m. We applied the Hunt (1999) model and the assumption of aquifer uniformity for calculating two-dimensional averaged time–drawdown data due to pumping only: $s(x, y, t) = s_Q(x, y, t)$ (Eqs. (4) and (11)). T was calculated with a constant saturated thickness of $m = 17$ m. Thus, the parameter vector comprises three fitting parameters to reproduce the observed drawdown, $s_{av}(x, y, t)$: the hydraulic conductivity, K, the aquifer storativity, S, and the unit streambed conductance K'/m'. The latter was calculated from Eq. (14) as follows: $K'/m' = \lambda/W$. We utilized late time–drawdown data only ($t > 1.25$ days), which are characteristic for the average hydraulic properties of a larger aquifer volume.

Data analyses were performed by linking the theoretical model to the model-independent nonlinear parameter optimizer PEST2000 (Doherty, 1994), which is based on a Gauss–Marquardt–Levenberg

algorithm to minimize the sum of squared differences (residuals) between calculated and measured data. We used the logarithmic transformation of the parameter vector, which strongly improved the convergence (Hill, 1998). To ensure that the global minimum of the sum of squared residuals function was reached, consecutive runs with varying initial parameter guesses were performed. Confidence limits that are calculated at the end of each optimization procedure are based on the linearization of the nonlinear models in the vicinity of the objective function minimum and are, thus, approximated values (Doherty, 1994).

5. Results

5.1. Measured time–drawdown data

Fig. 4 shows typical examples of three piezometer responses, $s(x, y, z, t)$ measured at different depths in the piezometers of cluster C2 located at the point bar. Each response exhibits the three distinct phases that are characteristic for drawdown under unconfined aquifer conditions (Neuman, 1975). Phase 1 is characteristic for the compressible aquifer properties and the borehole storage. A flattening of the time–drawdown curve occurs during the second phase, which is influenced by gravity drainage of the pore space above the declining water table. The third phase of the latest time–drawdown portion with a steeper slope typifies the average hydraulic properties of a larger aquifer volume and was utilized in our analyses ($t > 1.25$ days).

Inspection of the data from the piezometer cluster C5, C6, and C8 shows that the time–drawdown curves from the intermediate and deep piezometers intersect each other after about 30 min of pumping (see example in Fig. 5). Thereafter drawdown in the intermediate piezometer exceeds the drawdown in the deep piezometer, which causes vertical velocities at these clusters to converge towards intermediate aquifer depth suggesting a high conductivity inclusion (Kollet et al., 2002). The idea of a high conductivity heterogeneity was supported with slug test data in the piezometers with anomalous behavior. Also, analysis of the time–drawdown data from an additional pumping test performed at the same site without stream flow, under drought conditions in August, 2000, confirmed our findings and, additionally, revealed a spatial trend in the slopes of the late time–drawdown data. Generally, smaller slopes occurred at the point bar compared to larger slopes at the cut bank, which cannot be explained with the linear models for uniform aquifer conditions. We believe that aquifer heterogeneity is at least in part responsible for the observed deviations of the measured time–drawdown relationships from the theory.

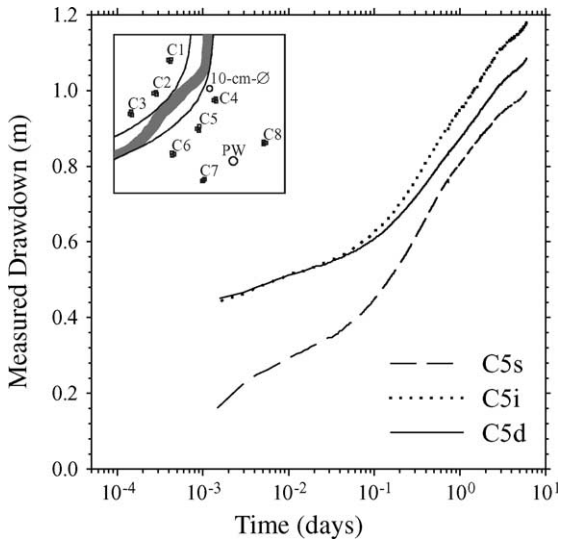

Fig. 5. Example of anomalous drawdown relationships between the intermediate and deep piezometers of the cluster C5.

In the following sections, results from the nonlinear parameter optimization are presented. We provide parameter estimates with approximated confidence limits, descriptive statistics, and some graphical analysis in order to facilitate the discussion. The correlation coefficient defined by Cooley and Naff (1990, p. 166) was used as a first proxy of goodness of fit throughout the different simulations. The value was always larger than 0.9 suggesting an acceptable fit between the calculated and measured data (Hill, 1998).

5.2. Individual clusters analyses

Descriptive statistics for the number of parameter values N, hydraulic conductivity K, streambed conductance K'/m', and storativity S from the ICA are shown in Table 2. Provided are the arithmetic

Table 2
Descriptive statistics from the ICA using a homogeneous aquifer model

Parameter	N	Grouping of Piezometer clusters						
		ICA				GCA	BCA	
		CV	Min	Max	Mean		Point bar	Cut bank
K (m/day)	8	0.57	102	350	195	94	36	126
K'/m' (day^{-1})	8	0.55	0.2	1.3	0.8	1.9	3.8	0.8
S (–)	8	0.47	0.01	0.06	0.07	0.16	0.10	0.07

Results from the BCA and GCA for a homogeneous aquifer are provided for comparison.

mean, minimum, maximum, and the coefficient of variation, CV, of the different parameters. Here, the arithmetic mean is only a tool to summarize the results and does not reflect the effective aquifer properties. Also provided are the parameter vectors from the BCA (point bar and cut bank), as well as from the GCA for comparison.

The ICA leads to large variations in all parameter estimates (Tables 2 and 3) that are reflected in large coefficients of variation, CVs (Table 2). Values for S are unreasonably low for a typical unconfined aquifer. The results also exhibit patterns in the estimates of K and K'/m', with much smaller K'/m' and larger K values at the point bar compared to the estimates from the cut bank ($K'/m' = 0.2–0.5$ day^{-1} and $K = 276–350$ m/day at the point bar versus $K'/m' = 0.7–1.3$ day^{-1} and $K = 102–153$ m/day at the cut bank).

These patterns lead to an unreasonably large difference between the streambed conductance coefficients, B_S, obtained from the interpretation of the drawdown data from the cut bank and the point bar ($\ell/B_S = 1.0\times10^{-2}–2.8\times10^{-2}$ at the point bar versus $\ell/B_S = 7.5\times10^{-2} - 2.2\times10^{-1}$ at the cut bank). Separately processed data from the 10-cm-diameter observation well exhibit a relatively small K and large K'/m'.

Christensen (2000) showed theoretically that the application of the Hunt model might lead to parameter correlation and/or insensitivity of drawdown to either the streambed conductance or the transmissivity depending on the observation location in the aquifer. This was also observed in our analysis and is reflected in the rather wide confidence limits of the individual parameter estimates (Table 3). However, nonlinear parameter estimation was verified by performing at

Table 3
Parameter vectors with confidence limits from the ICA using a homogeneous aquifer model

Data set		Parameter vector								
		K (m/day)			K'/m' (day^{-1})			S (–)		
		Estimate	95% confid. limits		Estimate	95% confid. limits		Estimate	95% confid. limits	
			Lower	Upper		Lower	Upper		Lower	Upper
Point bar	C1	348	315	384	0.3	0.2	0.5	0.05	0.04	0.06
	C2	276	246	309	0.5	0.3	0.7	0.05	0.04	0.06
	C3	350	313	392	0.2	0.1	0.4	0.03	0.02	0.04
Cut bank	C4	108	101	116	1.1	0.9	1.3	0.08	0.07	0.09
	C5	102	94	110	1.3	1.1	1.6	0.10	0.08	0.12
	C6	152	139	168	0.7	0.5	0.9	0.05	0.04	0.06
	C7	117	110	123	1.1	0.9	1.4	0.09	0.08	0.11
	C8	109	104	113	1.2	1.0	1.5	0.13	0.11	0.14
	10-cm	70	59	82	2.4	2.0	2.8	0.09	0.08	0.10

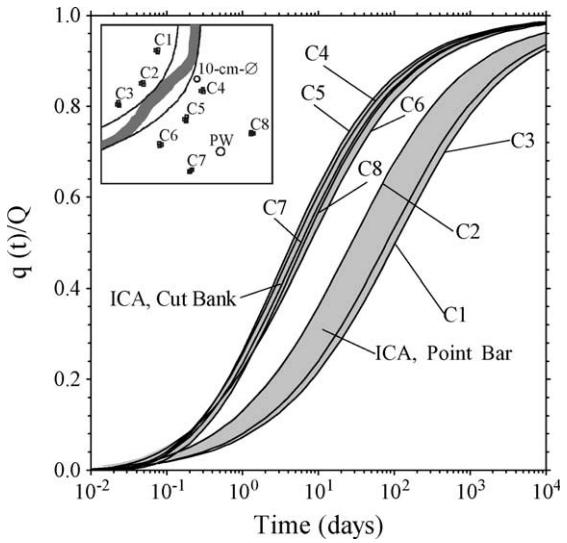

Fig. 6. Stream depletion rate curves calculated with the parameter vectors from the ICA. Each stream depletion rate curve corresponds to the parameter vector obtained from an individual cluster (Table 3). Shaded areas encompass the stream depletion rates estimated from piezometer clusters that are located at the different banks.

least two subsequent runs with different initial parameter guesses. These runs always converged at almost identical parameter vectors suggesting a unique solution.

Using these parameters, the stream depletion rates were assessed. Fig. 6 shows the dimensionless stream depletion curves calculated with the Hunt model using different parameter vectors obtained via the ICA. Large variations in the parameter estimates caused large uncertainty and differences in stream depletion predictions between individual curves. The pattern of spatial variations in K and K'/m' estimates is responsible for two distinct 'regions' (shaded areas) in Fig. 6. These regions are enveloped by the respective maximum and minimum stream depletion curves for the point bar and cut bank. Obviously, it is not possible to uniquely identify stream depletion rates for our stream–aquifer system from this graph without further data analysis.

5.3. Bank clusters analyses

Parameter estimates from the BCA are given in Table 4. The confidence limits reflect a possible decrease in parameter correlation and increase in the composite parameter sensitivity. Parameter estimates from the point bar and cut bank vary widely; in the case of K and K'/m' by a factor of about 3.5 and 4.7, respectively. The analysis of the data from the point bar yields the largest $K'/m' = 3.8\ \text{day}^{-1}$ compared to a value of $K'/m' = 0.81\ \text{day}^{-1}$ at the cut bank (Table 4).

Further comparison shows that the BCA results from the point bar differ from the ICA results for the clusters C1, C2, and C3 in Tables 2–4. Most importantly, all parameter values do not fall between the minimum and maximum parameter values of the point bar clusters C1, C2, and C3 obtained from the ICA. The BCA results from the cut bank reveal that S is also outside the range of values obtained from the ICA of the clusters C4, C5, C6, C7, and C8 (Tables 2–4).

Using the aquifer and streambed parameter estimates, the stream depletion rates were assessed. The difference between the hydraulic parameter

Table 4
Parameter vectors with confidence limits from the BCA for the point bar, the cut bank, and the GCA using a homogeneous aquifer model

Analysis	Data set	Parameter vector								
		K (m/day)			K'/m' (day^{-1})			S (–)		
		Estimate	95% confid. limits		Estimate	95% confid. limits		Estimate	95% confid. limits	
			Lower	Upper		Lower	Upper		Lower	Upper
BCA	Point bar (C1–C3)	36	29	44	3.8	3.6	4.0	0.10	0.09	0.11
	Cut bank (C4–C8)	126	121	131	0.8	0.7	0.9	0.07	0.06	0.08
GCA	C1–C8	93	90	97	1.9	1.6	2.1	0.16	0.13	0.20

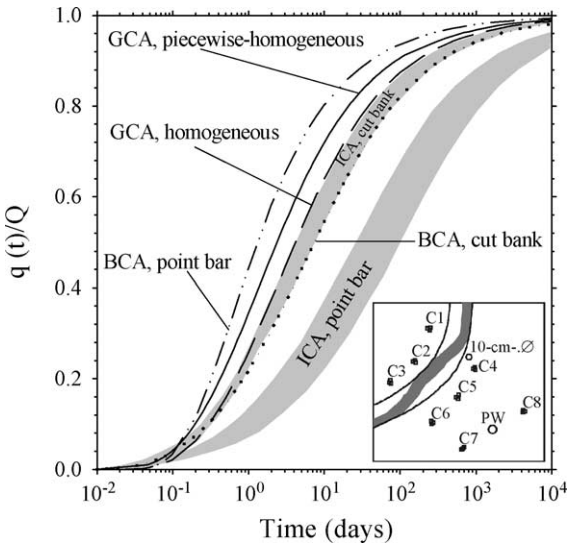

Fig. 7. Stream depletion rate curves calculated with the parameter vectors from the BCA of the different banks. The cut bank (C4 to C6) and point bar (C1 to C3) stream depletion curves are given by the dotted and dash-dotted lines, respectively. Stream depletion rate curves calculated with the parameter vectors from the GCA for homogeneous and piecewise-homogeneous aquifer conditions are given by the dashed and solid line, respectively. Shaded areas indicate stream depletion rates estimated from the ICA (Fig. 6).

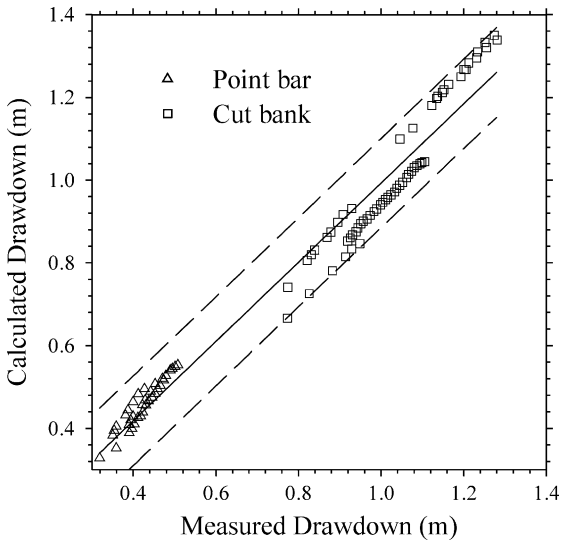

Fig. 8. Measured versus calculated drawdown from the GCA for a homogeneous aquifer. The linear regression line and the linear 95% prediction interval are indicated with the solid and dashed lines, respectively.

estimates obtained from the BCA and the ICA results obtained for the point bar is also clearly demonstrated by the dimensionless stream depletion rate curves shown in Fig. 7. The curves calculated with the parameter estimates obtained with the BCA of the point bar data lie outside the region defined by the simulated curves that use the results from the ICA of C1, C2, and C3. In contrast, results for the BCA from the cut bank data are consistent: the calculated curve falls in the region defined by the results from the ICA (clusters C4, C5, C6, C7, and C8).

5.4. Global clusters analysis

Tables 2 and 4 also contain the parameter estimates from the GCA and the respective confidence limits. These results fall within the bounds obtained from the BCA except for the aquifer storativity value. However, these results show that the parameter values disagree with the results from the ICA: the parameter values from GCA do not fall within the bounds of the parameter values obtained from the ICA (Table 2). This is also reflected in the stream depletion rate curves (Fig. 7).

The graph of calculated versus measured drawdown data using the parameter vector from the GCA is shown in Fig. 8. The overall match between

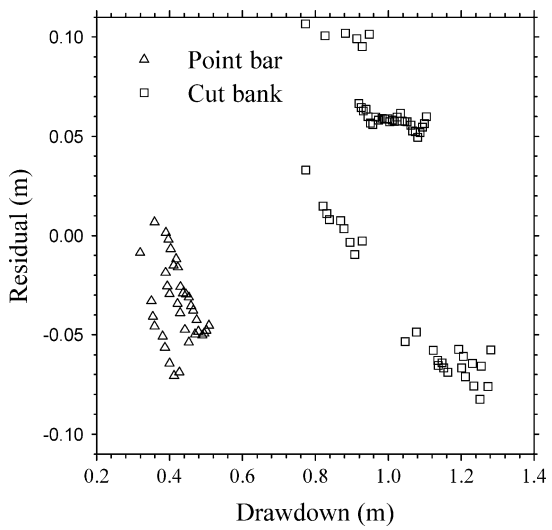

Fig. 9. Residuals versus drawdown plot from the GCA for a homogeneous aquifer.

the calculated and measured drawdown data appears to be reasonable, though a closer examination reveals that the model consistently over-predicts the slopes of the time–drawdown curves, in particular those involving the piezometer clusters at the point bar (C1, C2, and C3). This feature of the curve matches becomes more apparent from the residuals plot (Fig. 9) that reveals large and nonrandomly distributed residuals, indicating a low degree of goodness of fit (Poeter and Hill, 1997).

6. Discussion

The following results of the time–drawdown data analyses with linear uniform models require a more detailed discussion.

1. The large variance in parameter estimates obtained from the individual clusters analyses, ICA.
2. The inconsistency of the parameter estimates from the global, GCA, and bank, BCA, clusters analyses with the results from the ICA.
3. The low degree of goodness of fit between the calculated and measured drawdown data from the GCA.

These results suggest the violation of important assumptions made in the applied models, such as the assumption of aquifer homogeneity, the linearity and Dupuit assumptions, the simplified representation of the stream–aquifer interface, and the approximation of the stream as a straight line or strip. In the following sections, we discuss the influence of aquifer heterogeneity and the representation of the stream–aquifer interface in more detail.

We show that lateral aquifer heterogeneity may account for the spatial pattern in the parameter estimates from the point bar and cut bank. A combination of vertical and lateral aquifer heterogeneity might be responsible for large variances and the differences between the results from the GCA and ICA. The low degree of goodness of fit from the GCA indicates that the predictive capabilities of the theoretical models for drawdown and stream depletion rates are limited for the stream–aquifer system under consideration.

6.1. Inference of large-scale aquifer heterogeneity from time–drawdown data

6.1.1. Sedimentologic framework

Prairie Creek is a naturally meandering stream that migrates laterally, as follows from the inspection of topographical maps and field observations. The migration rate is determined by the erosional and depositional processes along the channel and depends upon the adjustment of the bed topography to varying flow conditions. During rising flow stages, erosion tends to occur in bend thalwegs along cut banks, that is, the river is eroding older sediments, which in our case are comprised of Quaternary alluvium deposited in paleochannels of the Platte River. As the flow stage is falling, reworked material is deposited in the channel forming fining-upward sequences with a basal coarse-grained layer. The layer of coarse-grained material also defines the interface between modern stream deposits and older alluvium. The depth of this interface is determined by the maximum depth of scour of the river, which is controlled by the bankfull width and river discharge (Allen, 1970; Bridge and Jarvis, 1976; Bridge, 1977; Bridge et al., 1995; Fraser and Davis, 1998). Channel migration and translation associated with erosion and deposition lead to the development of point bars. A conceptual cross-section is shown in Fig. 10.

The hydrogeologic implications can be summarized as follows. The deposited reworked material has different properties than the alluvium undergoing erosion. Thus, there exist at least two zones, Zone A and Zone B, in Fig. 10 with distinctly different

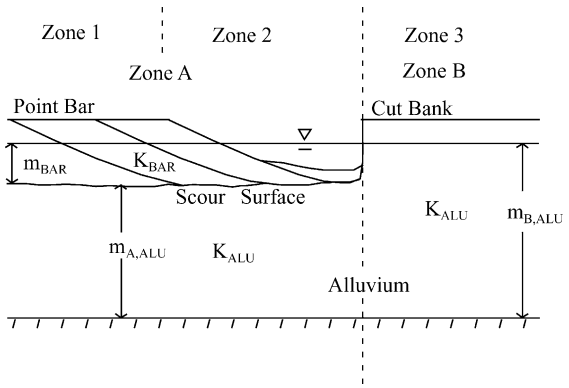

Fig. 10. Conceptual hydrostratigraphic cross-section. The zoning of the piecewise-homogeneous BZT model is indicated at the top.

effective hydraulic conductivity values K_A and K_B. This nonuniformity has a major influence on the pumping-induced drawdown. Assuming only two-dimensional groundwater flow and isotropic conditions, the effective hydraulic conductivity and transmissivity of Zone A and Zone B are

$$K_A = \frac{K_{BAR} m_{BAR} + K_{ALU} m_{A,ALU}}{m_{BAR} + m_{A,ALU}}, \quad (21)$$

$$K_B = K_{ALU},$$

$$T_A = K_A (m_{BAR} + m_{A,ALU}), \quad (22)$$

$$T_B = K_{ALU} m_{B,ALU},$$

where K_{BAR} and K_{ALU} are the hydraulic conductivity values of the point bar deposits and the Quaternary alluvium, respectively; m_{BAR}, $m_{A,ALU}$, and $m_{B,ALU}$ are the saturated thickness of the point bar deposits and the Quaternary alluvium of Zone A and B, respectively.

The BZT model offers the option of dividing the aquifer into three zones that are infinitely long straight strips of different hydraulic conductivity and storativity. We exploit this option based on the described sedimentologic and hydrologic rationales.

6.1.2. Parameter identification using the BZT model

In the most general case, the use of the BZT model requires seven fitting parameters that include T_i, S_i, and K'/m', where $i = 1, 2,$ and 3. However, this number can be reduced, because Zlotnik and Huang (1999) have shown that compressibility of Zone 2 has no significant influence on the solution. In addition, a difference in S_i between Zones 1 and 3 can be neglected by physical considerations.

Therefore, the parameter vector used in the analysis includes the three different hydraulic conductivities, K_1, K_2, and K_3 of the Zones 1, 2, and 3, the storativity, $S_{1,3} = S_1 = S_3$ that is assumed to be constant in the Zones 1 and 3, and the unit streambed conductance, K'/m'. The storativity of Zone 2 was held constant at a value of $S_2 = 10^{-3}$. The transmissivity of each zone (T_1, T_2, and T_3) was calculated with a constant average saturated thickness of $m_i = 17$ m, $i = 1, 2,$ and 3. Thus, the parameter vector contained five components.

The parameter identification results are summarized in Table 5. The nonlinear parameter estimation process converges at a parameter vector that is consistent with the presented sedimentologic rationale of piecewise-homogeneous aquifer conditions. The hydraulic conductivity of Zones 1 and 2 were found to be almost identical: $K_A = K_1 = K_2 = 22$ m/day (Table 5). The hydraulic conductivity of Zone 3 is $K_B = K_3 = 115$ m/day, which leads to a K-ratio between the Zones 1 (or 2) and 3 of $K_3/K_1 = K_3/K_2 \approx 5.2$. The relatively wide confidence limits of the K_1-estimate stem from the high correlation of this parameter with K_2 and K'/m'. Yet, runs with different initial guesses converged at almost the same result.

In the next step, fitting parameters K_1 and K_2 were replaced by a single parameter $K_1 = K_2 = K_A$. The resulting second parameter vector with four components led to a decrease in parameter correlation compared to the previous results (Table 5). Also, Figs. 11 and 12 show a strong improvement

Table 5
Parameter vectors with confidence limits from the GCA using a piecewise-homogeneous aquifer model

N	Parameter vector														
	K_1 (m/day)			K_2 (m/day)			K_3 (m/day)			K'/m' (day^{-1})			$S_{1,3}$ (–)		
	Estimate	95% confid. limits		Estimate	95% confid. limits		Estimate	95% confid. limits		Estimate	95% confid. limits		Estimate	95% confid. limits	
		Lower	Upper		Lower	Upper		Lower	Upper		Lower	Upper		Lower	Upper
5	22	9	52	21	19	24	115	111	118	2.2	2.0	2.5	0.14	0.13	0.16
4	21	19	23	$K_1 = K_2 = K_A$			115	112	118	2.3	2.2	2.4	0.14	0.13	0.15

N is the number of fitting parameters.

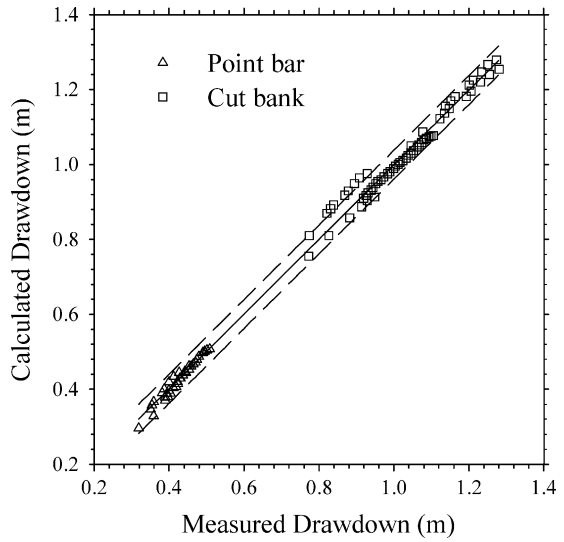

Fig. 11. Measured versus calculated drawdown from the GCA for a piecewise-homogeneous aquifer. The linear regression line and the 95% prediction interval are indicated with the solid and dashed lines, respectively.

in the results, including a higher degree of goodness of fit between the measured and calculated data and more randomly distributed and smaller residuals.

These results indicate that the time–drawdown behavior can be consistently explained and analyzed by incorporating hydrostratigraphic considerations

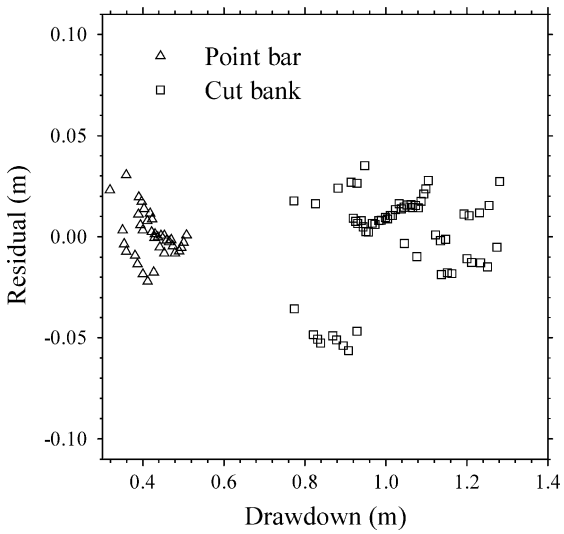

Fig. 12. Residuals versus drawdown from the GCA for a piecewise-homogeneous aquifer.

that are based on well-established sedimentologic concepts into an appropriate BZT model. Though $K_1 = K_2 = K_A$ appears to be at the lower parameter bound for the hydraulic conductivity at the point bar, the determined hydraulic conductivity distribution agrees well with the hydraulic conductivity from the slug tests, K_{slug} ($K_{slug} = 24–120$ m/day at the point bar versus $K_{slug} = 22–290$ m/day at the cut bank). A storativity value of $S = 0.14$ is smaller than expected from drainage experiments, but it is consistent with data from other pumping tests in unconfined aquifers (Neuman, 1975; Nwankwor et al., 1984; Moench, 1994).

6.2. Evaluation of stream depletion considering large-scale heterogeneity

A stream depletion rate curve was generated using the parameter vector obtained from the GCA using the piecewise-homogeneous aquifer model (Fig. 7). This curve falls between the curves calculated using the parameter values from the cut bank and the point bar from the BCA.

The ultimate goal is the prediction of the stream depletion rate from the analyses of pumping test data. As it follows from previous discussion, such predictions are interpretation-dependent and fraught with uncertainty. However, the results from the BCA and GCA define a relatively narrow domain of stream depletion predictions, after discarding the ICA results due to patterned differences and wide confidence limits. That leads to a better constraint of stream depletion estimates, though some uncertainty in stream depletion rates still remains.

During the pumping test, streamflow measurements where performed in an attempt to determine stream depletion rates independently and constrain our estimates. Yet, large measurement errors (~5–10%) inherent in modern gauging techniques for natural streams make an objective interpretation of the collected data difficult.

6.3. On the physical meaning of streambed conductance

The presented sedimentologic rationale lends little credibility to the simplified concept of streambed conductance (Section 6.1.1). At our site, use of this

concept yields results that cannot be reconciled with available data from independently performed streambed characterization based on small-scale injection tests and applications of ground-penetrating radar (Cardenas and Zlotnik, 2003). Indeed, use of $K'/m' = 2.25\ \text{day}^{-1}$ from Table 5 and effective streambed hydraulic conductivity $K' = 18$ m/day by Cardenas and Zlotnik (2003) yields an effective streambed thickness of $m' = 8$ m. This estimate of streambed thickness is unreasonably large for our specific stream–aquifer system and is in variance with the concept of a "thin semi-pervious" layer. However, the good agreement of the K'/m'-values inferred from the different models (homogeneous versus piecewise-homogeneous) is surprising (Tables 4 and 5).

Kollet et al. (2002) have shown that there exist large vertical hydraulic gradients and complex three-dimensional flow patterns in the aquifer and near stream zone that might violate the Dupuit and linearity assumptions. In addition, geometric features of the stream channel, such as variations in the width, the wetted perimeter, and channel sinuosity are not taken into account.

Our results indicate that K'/m' might not represent a semi-pervious streambed of finite thickness and uniform hydraulic conductivity. In our case, this parameter is better interpreted as a convenient lumped factor that empirically accounts for three-dimensional groundwater flow, anisotropy in the hydraulic conductivity, and geometric features of the stream–aquifer system that are not considered in the analytical models. Therefore, the transfer of the streambed conductance values estimated from two-dimensional models to numerical models with a more realistic three-dimensional representation of the hydraulic and geometric properties will require case-specific revisions.

7. Summary and conclusions

We investigated the applicability of pumping test data analysis with linear two-dimensional models for obtaining the aquifer and streambed hydraulic parameters and stream depletion rates. The unique design of this study explicitly considered the actual three-dimensional flow structure. In May 2000, a pumping test was performed in a well located at a distance of about 57 m from the stream. Drawdown data were collected in eight piezometer clusters, each with three piezometers screened at shallow, intermediate, and deep aquifer depth. After vertical averaging the measured drawdown at each cluster, the data were analyzed in the following groups: individual piezometer clusters; all clusters on the point bar; all clusters on the cut bank; and all piezometer clusters.

Application of the uniform aquifer model (Hunt, 1999) resulted in a large variability and spatially patterned differences in parameter estimates and thus, uncertain stream depletion rate predictions. Moreover, curve matches between the measured and calculated data frequently revealed a low degree of goodness of fit. The above deficiencies in the results were attributed to the lateral and also vertical aquifer heterogeneity.

We supported our reasoning with the analyses of vertical head gradients in piezometer clusters and with slug test data, and discussed the use of a piecewise-homogeneous aquifer model based upon the sedimentologic rationale of the meandering stream architecture (cut bank versus point bar). Application of the BZT model (Butler et al., 2001) resulted in an improvement in the goodness of fit between the measured and calculated data, as well as a decrease in the uncertainty of stream depletion rate predictions.

The results from our analyses and the hydrostratigraphy at the test site suggest that aquifer heterogeneity is the major cause for the inconsistencies in parameter estimates and stream depletion predictions. The concept of streambed conductance appears to be a too simplified approximation of the hydraulic connection between the stream and the aquifer in our hydrogeologic setting.

At this stage, parameter identification and stream depletion predictions with linear uniform models of stream–aquifer interactions are fraught with uncertainties. We recommend the analysis of the drawdown data in different groups and detailed inspection of the time–drawdown behavior and curve matches with the theoretical models. This might help in identifying shortcomings of the applied models. Incorporation of large-scale aquifer heterogeneity via piecewise-homogeneous models that are based on sedimentologic concepts of the stream–aquifer system under

consideration might improve parameter estimates and decrease the uncertainty in stream depletion rate predictions.

These results imply that more than one piezometer or piezometer cluster is needed for parameter estimation with following stream depletion rate evaluation. In general, we recommend the installation of several clusters on each stream bank.

Accurate stream flow measurements might serve as a useful constraint for stream depletion predictions. In naturally flowing rivers, however, they are difficult to obtain under typical discharge conditions.

Future investigations should include the impact of the linearity assumptions, the conceptual representation of the stream–aquifer interface, the approximation of the stream as a straight line or strip, and the influence of regional ambient flow upon stream depletion predictions.

Acknowledgements

This research was supported by the USGS Regional Water Resources Competitive Grants Program grant 1434Hq96Gr02683, 1998–2001; grants from the Central Platte Natural Resources District, Nebraska, 1999–2002; and the Water Center, University of Nebraska-Lincoln. The authors acknowledge D. Woodward, Central Platte Natural Resources District, Nebraska, for assistance with the project management and equipment; and R.J. Edmison for providing access to the site and equipment for the performance of the pumping tests in the years 1999 to 2000. Comments from M. Bakker, K. Jeongkon, and one anonymous reviewer substantially improved the manuscript.

References

Allen, J.R.L., 1970. A quantitative model of grain size and sedimentary structures in lateral deposits. Geol. J. 7 (1), 129–146.

Anderson, M.P., Woessner, W.W., 1992. Applied Groundwater Modeling: Simulation of Flow and Advective Transport, Academic Press, San Diego, pp. 281.

Bredehoeft, J., 1997. Safe yield and the water budget myth. Ground Water 35 (6), 929.

Bridge, J.S., 1977. Flow, bed topography, grain size, and sedimentary structure in open channel bends: a three-dimensional model. Earth Surf. Processes 2, 401–416.

Bridge, J.S., Jarvis, J., 1976. Flow and sedimentary processes in the meandering river South Esk, Glen Clova, Scotland. Earth Surf. Processes 1 (4), 303–336.

Bridge, J.S., Alexander, J., Collier, R.E.Ll., Gawthorpe, R.L., Jarvis, J., 1995. Ground penetrating radar and coring used to study the large-scale structure of point-bar deposits in three dimensions. Sedimentology 42, 839–852.

Butler, J.J. Jr, Tsou, M.S., 1999. The StrpStrm Model for calculation of pumping induced drawdown and stream depletion. Kansas Geol. Survey Computer Ser. Rep. 99-1.

Butler, J.J., Zlotnik, V.A., Tsou, M.S., 2001. Drawdown and stream depletion produced by pumping in the vicinity of a finite-width stream of shallow penetration. Ground Water 39 (5), 651–659.

Cardenas, M.B.R., Zlotnik, V.A., 2003. Three-dimensional model of modern channel bend deposits. Water Resour. Res. 39 (6), 1141, doi: 10.1029/2002WR001383, 2003.

Christensen, S., 2000. On the estimation of stream flow depletion parameters by drawdown analysis. Ground Water 38 (5), 726–734.

Conrad, L.P., Beljin, M.S., 1996. Evaluation of an induced infiltration model as applied to glacial aquifer systems. Water Resour. Bull., Am. Water Res. Ass. 32 (6), 1209–1219.

Cooley, R.L., Naff, R.L., 1990. Regression modeling of groundwater flow: US Geological Survey Techniques in Water-Resources Investigations. Book 3, Chapter B4, 232 p.

Doherty, J., 1994. PEST-model-independent parameter estimation, Watermark Computing, Corinda, Australia, pp. 122.

Fraser, G.S., Davis, J.M. (Eds.), 1998. Hydrogeologic Models of Sedimentary Aquifers, Society of Sedimentary Geology, Tusla, Oklahoma, p. 188.

Glover, R.E., Balmer, C.G., 1954. River depletion resulting from pumping a well near a river. Eos Trans. Am. Geophys. Union 35, 468–470.

Hantush, M.S., 1965. Wells near streams with semipervious beds. J. Geophys. Res. 70, 2829–2838.

Hill, M.C., 1998. Methods and guidelines for effective model calibration. US Geological Survey, Water-Resources Investigation Report 98-4005, pp. 90.

Hunt, B., 1999. Unsteady stream depletion from ground water pumping. Ground Water 37 (1), 98–102.

Hunt, B., Weir, J., Clausen, B., 2001. A stream depletion field experiment. Ground Water 39 (2), 283–289.

Jenkins, C.T., 1968. Techniques for computing rate and volume of stream depletion by wells. Ground Water 6 (2), 37–46.

Kollet, S.J., Zlotnik, V.A., Woodward, D., 2002. A field and theoretical study on stream–aquifer interactions under pumping conditions in the Great Plains, Nebraska. Am. Water Res. Ass., Proc., July 2002, 29–34.

Moench, A.F., 1994. Specific yield as determined by type-curve analysis of aquifer-test data. Ground Water 32 (6), 949–957.

Moore, J.E., 1966. An evaluation of the effect of groundwater pumpage on the infiltration rate of a semipervious streambed. Water Resour. Res. 2 (4), 691–696.

Neuman, P.T., 1975. Analysis of pumping test data from anisotropic unconfined aquifers considering delayed gravity response. Water Resour. Res. 11 (2), 329–342.

Nwankwor, G.I., Cherry, J.A., Gillham, R.W., 1984. A comparative study of specific yield determination for a shallow sand aquifer. Ground Water 22 (6), 764–772.

Nyholm, T., Christensen, S., Rasmussen, K.R., 2002. Flow depletion in a small stream caused by ground water abstraction from wells. Ground Water 40 (4), 425–437.

Peckenpaugh, J.M., Dugan, J.T., 1983. Hydrogeology of parts of the Central Platte and Lower Loup Natural Resources Districts, Nebraska. US Geological Survey, Water-Resources Investigation, 83-4219, pp. 100.

Poeter, E.P., Hill, M.C., 1997. Inverse models: a necessary next step in ground-water modeling. Ground Water 35 (2), 250–260.

Sniegocki, R.T., 1955. Ground-water resources of the Prairie Creek Unit of the lower Platte River basin, Nebraska. Geological Survey Water-Supply Paper 1327, pp. 133.

Sophocleous, M., 1997. Managing water resources systems: why safe yield is not sustainable. Ground Water 35 (4), 561.

Sophocleous, M., Townsend, M.A., Vogler, L.D., McClain, T.J., Marks, E.T., Coble, G.T., 1988. Experimental studies in stream–aquifer interaction along the Arkansas river in central Kansas—field testing and analysis. J. Hydrol. 98, 249–273.

Sophocleous, M., Koussis, A., Martin, J.L., Perkins, S.P., 1995. Evaluation of simplified stream–aquifer depletion models for water rights administration. Ground Water 33 (4), 579–588.

Spalding, C.P., Khaleel, R., 1991. An evaluation of analytical solutions to estimate drawdowns and stream depletion by wells. Water Resour. Res. 27 (4), 597–609.

Theis, C.V., 1941. The effect of a well on the flow of a nearby stream. Eos Trans., Am. Geophys. Union 22, 734–738.

Zlotnik, V.A., Huang, H., 1999. Effect of shallow penetration and streambed sediments on aquifer response to stream stage fluctuations (analytical model). Ground Water 37 (4), 599–605.

Zlotnik, V.A., Huang, H., Butler Jr., J.J., 1999. Evaluation of stream depletion considering finite stream width, shallow penetration, and properties of streambed sediments. In Proceedings of Water 99, Joint Congress, Brisbane, Australia, pp. 221–226.